The removal of diuron from agricultural wastewaters by *Trametes versicolor* immobilized on pinewood in simple channel reactors

Eduardo Beltrán-Flores[a], Josefina Torán[a], Glòria Caminal[b], Paqui Blánquez[a, *], Montserrat Sarrà[a].

[a] Departament d'Enginyeria Química Biològica i Ambiental, Escola d'Enginyeria, Universitat Autònoma de Barcelona, 08193 Bellaterra, Barcelona, Spain.

[b] Institut de Química Avançada de Catalunya (IQAC) CSIC, Jordi Girona 18-26, 08034 Barcelona, Spain.

[*] Corresponding author. E-mail address: Paqui.Blanquez@uab.cat (P. Blánquez)

Abstract

The presence of pesticides in agricultural wastewater entails harmful risks to both the environment and public health. In this study, two channel-type bioreactors with *Trametes versicolor* immobilized on pinewood chips were evaluated in terms of the removal efficiency of diuron from agricultural wastewater under non-sterile conditions. First, both single and successive sorption processes of diuron on pinewood chips were evaluated. The Freundlich model showed the best correlation in the sorption isotherm study (R^2 = 0.993; Δq = 5.245), but according to repeated sorption experiments, the Langmuir model (R^2 = 0.993; Δq = 5.757) was considered more representative. Equilibrium was reached after approximately 48 h, and the Elovich kinetic model gave the best fit with the experimental data. A packed-bed channel bioreactor (PBCB) was found to be a remarkable alternative able to remove up to 94 % diuron from agricultural wastewater during 35 d. However, periodic manual mixing was required to guarantee an aerobic process, and a rotating drum bioreactor (RDB) was subsequently proposed as an enhanced version. The RDB removed up to 61 % diuron during 16 d using almost 7 times lower wood dose (152 g wood·L^{-1}) than in the PBCB (1000 g wood·L^{-1}).

Keywords:

Bioreactor, pesticide, low-cost sorbent, organic contaminant, fungal treatment

1. Introduction

Diuron is the common name of N-(3,4-dichlorophenyl)-N,N-dimethyl-urea, which is a phenyl urea herbicide extensively used to control germinating grass, broadleaf weeds and mosses. This compound inhibits photosynthesis by blocking electron transfer in photosystem II in a broad spectrum of plants and photosynthetic microorganisms. Diuron is applied to many crops, especially cereals, but also in non-agricultural areas for the maintenance of railways, gardens, roads, parks, etc. (Giacomazzi and Cochet,

2004; Tixier et al., 2001).

The use of diuron can lead to serious environmental and public health problems due to its high persistence and toxic effects on living beings. Diuron has a recalcitrant structure with a half-life of approximately 328 d in soil (Jury et al., 1983). Once applied to the target field, rainfall can deliver diuron through runoff and leaching from the ground to nearby water bodies (Langeron et al., 2014; Rupp et al., 2006). Aquatic organisms are especially susceptible to diuron exposure, but studies on animals have also revealed carcinogenic effects of diuron on rats and cytotoxic and potentially genotoxic damage in human cells (Huovinen et al., 2015).

The United States Environmental Protection Agency has also identified diuron as a "known/likely" human carcinogen considering several types of carcinomas developed in rats (US EPA, 2003). Diuron has been included in the list of Priority Substances in the Field of Water Policy of the European Commission Directive 2000/60/EC (European Commission, 2000). This directive urges the Member States to progressively reduce the emission and release of such substances. It also demands compliance with the European Commission Directive 98/83/CE, which requires Member States to meet the concentration limit of 100 $ng \cdot L^{-1}$ for individual species of pesticides in water intended for human consumption (European Commission, 1998). Accordingly, declining trends in diuron concentrations have been detected in some areas(Palma et al., 2014), probably partly due to the EC decision (Commission Decision 2007/417/EC) not to include diuron in Annex I of Directive 91/414/EEC for authorized phytosanitary products in the EU (European Commission, 2007). However, high concentrations have been recently detected in natural water resources (Lapworth and Gooddy, 2006), especially near crop fields and after rainfall, reaching values up to 150 $ng \cdot L^{-1}$ (Ccanccapa et al., 2016).

Conventional activate sludge process in wastewater treatment plants (WWTPs) is not specifically designed to completely remove most pesticides [14]. In fact, poor removal

efficiencies (46.0 ± 16.3 %) have been typically obtained for diuron in WWTPs. Several alternative treatments have been proposed to address these kinds of recalcitrant compounds. They are commonly classified into physical, chemical and biological treatments according to their elimination strategy. The first two groups of treatments are frequently presented together as physico-chemical treatments due to the strong relationship between these phenomena. Physico-chemical treatments mainly include adsorption, advanced oxidation processes (ozonation, photocatalysis, etc.) and membrane filtration (Marican and Durán-Lara, 2018). However, these technologies can be unfeasible for treating micropollutants from wastewater since they can require expensive regeneration processes, high energy or catalyst consumption, and additional post-treatments of the rejected streams (Prieto-Rodriguez et al., 2012; Taheran et al., 2016) .

Among biological treatments, bioremediation using white-rot fungi (WRF) has been proposed as a promising alternative to degrade a wide range of xenobiotics, such as pharmaceutically active compounds (Haroune et al., 2014), polycyclic aromatic hydrocarbons (Ding et al., 2013), personal care products (Rodarte-Morales et al., 2011), endocrine-disrupting chemicals (Cabana et al., 2007) and pesticides (Mir-Tutusaus et al., 2014). In particular, *Trametes versicolor* is a fungus of special interest for bioremediation purposes since it has an unspecific enzymatic system composed of a family of ligninolytic extracellular enzymes (laccase and lignin, manganese and versatile peroxidases) and the intracellular enzymatic system known as cytochrome P450 (Asgher et al., 2008).

Despite the great potential of WRF, there is a critical drawback that can complicate its implementation on an industrial scale. Treating real wastewater matrices under nonsterile conditions negatively influences the enzymatic activity and survival of the fungus due to pressure exerted by other microorganisms, mainly bacteria. Operating

under nonsterile conditions normally leads to shorter operation times and declines in degradation performance (Mir-Tutusaus et al., 2016).

Different strategies have been adopted to favour the predominance of fungi against bacteria, such as biomass renovation (Blánquez et al., 2006), adjustment of the C/N ratio and pH (Badia-Fabregat et al., 2016), and fungus immobilization (Li et al., 2015), among others. There are two types of immobilization strategies: autoimmobilization (fungal pellets) and immobilization onto supports (Mir-Tutusaus et al., 2018). In particular, immobilization on natural substrates, such as wood from timber industry wastes, presents outstanding possibilities since such substrates can be used as low-cost supports without adding any other source of nutrients. Wood substrates have a complex structure that is highly resistant to bacterial attack. This structure is especially convenient for the treatment of wastewater with a low organic content, such as agricultural wastewaters, in which the addition of external nutrients is typically mandatory (Torán et al., 2017).

The aim of this work was to study different channel-type bioreactors with pinewood chips colonized by *T. versicolor* designed to remove diuron from real wastewater under non-sterile conditions. For that purpose, sorption onto pinewood was first analysed by both isotherm models and kinetics studies in batch mode and successive batch sorption experiments. Then, wastewater spiked with diuron was treated in a simple packed-bed channel bioreactor (PBCB) under non-sterile conditions. Finally, a rotating drum bioreactor (RDB) incorporating automatic agitation was studied as an enhanced version of the PBCB.

2. Materials and methods

2.1. Lignocellulosic material

Pinewood pallets were kindly provided by Timgad S.A. (Barcelona, Spain). The pinewood pallets were fragmented into small pieces using a STERWINS Esh1-40.3 2500 W crushing machine. The obtained wood chips were sieved through two standardized meshes of 16 and 7.10 mm, selecting the middle fraction. The resulting wood chips were completely submerged in tap water and autoclaved at 120 ºC for 30 min, to later discard the free water.

The bulk density of the wood (ρ_b) was calculated according to the standardized method ASTM D7481 – 18 (ASTM, 2018). The volume occupied by 50 g of wood chips (m_s) was measured in a 500 mL graduated cylinder. Then, the bulk density was obtained using Eq. (1).

$$\rho_b = \frac{m_s}{V_b} \quad (1)$$

To calculate the bed porosity of the wood chips, a defined mass of tap water (m_w), which was converted into volumetric units (V_w), was poured into the graduated cylinder until the wood chips were completely submerged. The bed porosity was calculated by Eq. (2).

$$\phi = \frac{V_w}{V_b} \quad (2)$$

2.2. Agricultural wastewater

Wastewater samples were collected from an agricultural drainage channel in the Llobregat River Basin (Catalonia, Spain). These samples were collected in two different periods of time, for the PBCB experiments in June 2017, and for the sorption and the RDB experiments in September 2018. The agricultural wastewater was spiked with 6 ppm, 8 ppm and 10 ppm diuron for the single batch, successive sorption and bioremediation experiments, respectively. The wastewater was stored at 4 ºC.

2.3. Chemicals and reagents

142 Diuron was purchased from Sigma Aldrich (Barcelona, Spain). Malt extract was
143 acquired from Scharlau (Barcelona, Spain). High-performance liquid chromatography
144 (HPLC) grade acetonitrile was supplied by Merck (Darmstadt, Germany). All chemical
145 used were of high purity grade.

146 **2.4. Fungal strain and culture conditions**

147 *T. versicolor* (ATCC 42530) was purchased from the American Type Culture Collection.
148 The fungus was maintained by subculturing in agar plates of malt extract (2 % w/v) at
149 25 °C every 30 d. A mycelial suspension of *T. versicolor* was prepared according to
150 Blánquez et al. (Blanquez et al., 2004).

151 The prepared mycelial suspension of *T. versicolor* was inoculated on the wood chips
152 (0.25 mL mycelial suspension·g wood^{-1}) inside a polyvinyl chloride box covered with
153 aluminium foil. Cultures were incubated during 9 and 20 d at 25 ºC before the PBCB
154 and RDB treatments, respectively.

155 **2.5. Sorption and kinetic studies**

156 Various amounts of pinewood sorbent (5, 10, 20, 30, 40 and 60 g) were added to a
157 series of 1 L Erlenmeyer flasks that were previously filled with 200 mL spiked
158 wastewater. Spiked wastewater was initially adjusted to pH 4.5. A continuous orbital
159 agitation of 135 rpm and a constant temperature of 25 ºC were maintained for almost 3
160 d (70 h) until equilibrium was reached. The remaining pesticide concentrations were
161 analysed by HPLC in defined intervals of time.

162 Eq. (3) and Eq. (4) were used to calculate diuron sorption at any time t and at
163 equilibrium respectively:

164 $$q_t = \frac{(C_0 - C_t)\,V}{m} \quad (3)$$

$$q_e = \frac{(C_0 - C_e)\,V}{m} \quad (4)$$

where C_0, C_t and C_e (mg·L^{-1}) are the diuron concentrations at initial time, any specific time t, and at equilibrium respectively, V (L) is the solution volume and m (g) is the wood mass used in each experiment.

Successive sorption cycles were performed by repeating the batch mode experiment for m = 20 g of wood. The wood chips were strained at the end of each cycle to be later reused in the following batches. The same C_0 and operating conditions were maintained in all cycles.

2.6. Packed bed channel bioreactor

The PBCB was constructed with a polyvinylchloride gutter (length x diameter: 50.5 x 11 cm). Two channels were operated in parallel: the control one with pinewood, and the inoculated one with pinewood colonized with *T. versicolor*. In both cases, 1 kg wood and 1 L wastewater were used (dose of 1000 g·L^{-1}). A hydraulic retention time (HRT) of 3 d was employed.

The PBCB inlet and outlet were located at each of the reactor sides. Two different experiments were performed using the PBCB: one PBCB experiment with spiked tap water (10 ppm) and another PBCB experiment with spiked wastewater (10 ppm). Wastewater was continuously pumped from the influent tank, which was mixed by a magnetic stirrer, to the reactor, and then pumped out to the effluent tank. Samples were collected from the effluent tank, and filtered and analysed by HPLC as described in Section 2.8. The pH was initially adjusted to 4.5 and monitored at different points of the system. No additional substrate or nutrient was added to the reactor.

2.7. Rotating drum bioreactor

The RDB was constructed using the same polyvinylchloride channel presented in Section 2.6. However, an additional inner tube of methacrylate was located in the center of the longitudinal axis of the channel. The wood chips were placed inside the internal tube, while the wastewater was contained inside the channel. The tube was provided with multiple holes of 8 mm diameter to allow the contact between the wood chips and the wastewater. Approximately 30 % of the internal tube volume was submerged in the liquid phase, while the remaining volume was in direct contact with the air. The inner tube was connected to a 12 V electric motor (Worm Gear Motor; model: 4632-370) that was operated at a constant rotation speed of 6 rpm. The wastewater was continuously pumped from the influent tank to one RDB side, and the effluent stream was drained by overflow from the other RDB side. The RDB was equipped with a pH controller to adjust the pH between 4.3 – 4.7 by adding either 1 M HCl or 1 M NaOH when required. The system was continuously operated with an HRT of 3 d.

2.8. Pesticide analysis from liquid phase

1 mL liquid samples were periodically taken from the effluent tanks, filtered through Millipore Millex-GV PVDF filters of 0.22 µm and introduced in amber vials for HPLC analysis. A Dionex Ultimate 3000 HPLC was used to determine diuron concentrations of the liquid samples. The HPLC was equipped with a UV detector working at 254 nm. The separation was performed in a C18 reversed-phase column (Phenomenex®, Kinetex® EVO C18 100 Å, 4.6 mm × 150 mm, 5 µm) at constant 30 ºC. The initial composition of the mobile phase was 35 % acetonitrile and 65 % solution of 0.1 % formic acid in MilliQ water. Then, the acetonitrile composition raised in ramp to 45 % during the first 15 min. A total sample volume of 40 µL was injected at a constant flow rate of 0.8 $mL \cdot min^{-1}$.

2.9. Routine analysis

Laccase activity was determined through the oxidation of 2.6-Dimethoxyphenol (DMP) by laccase enzyme (Cruz-Morató et al., 2013). The absorbance was measured by a UNICAM 8625 UV/VIS spectrometer at 650 nm, and the conductivity was analysed using a CRISON MicroCM 2100 conductometer. The heterotrophic plate count (HPC) was measured per triplicate according to the APHA standard (APHA, 1995). The chemical oxygen demand (COD) and the ammonia concentration were determined through commercial kits LCK114 or LCK314m and LCH303, respectively (Hach Lange, Germany).

2.10. Isotherm and kinetic equations

The Langmuir, Freundlich and Temkin isotherm models are expressed by Eq. (5-8):

Langmuir equation: $$q_e = \frac{q_{max} K_L C_e}{1 + K_L C_e} \quad (5)$$

Freundlich equation: $$q_e = K_F C_e^{1/n} \quad (6)$$

$$K_F = \frac{q_{max}}{C_0^{1/n}} \quad (7)$$

Temkin equation: $$q_e = B \ln(A C_e) \quad (8)$$

where q_e is the sorbed diuron per gram of wood ($mg \cdot g^{-1}$) at equilibrium, q_{max} the Langmuir maximum sorption capacity ($mg \cdot g^{-1}$), K_L the sorption energy ($L \cdot mg^{-1}$), C_e the diuron concentration at equilibrium ($mg \cdot L^{-1}$), K_F the sorption capacity (units depend on n), C_0 the initial diuron concentration ($mg \cdot L^{-1}$), n the intensity of the sorption (unitless), and B = RT/A, being R the ideal gas constant (8.314 $J \cdot mol^{-1} \cdot K^{-1}$), T the temperature (K) and A is the Temkin equilibrium constant ($L \cdot mg^{-1}$).

Pseudo-first, pseudo-second, Elovich and intra-particle diffusion (IPD) kinetic equation are shown in Eq. (9-12).

Pseudo-first order equation: $$q_t = q_e\left(1 - e^{-k_1 t}\right) \quad (9)$$

Pseudo-second order equation: $q_t = \frac{k_2 q_e^2 t}{1+k_2 q_e t}$ (10)

Elovich equation: $q_t = b \ln(abt)$ (11)

Intra-particle diffusion equation: $q_t = K_{id} t^{1/2} + C$ (12)

where q_t is the diuron sorbed per gram of wood ($mg \cdot g^{-1}$) at any time t (h), k_1 is the pseudo-first rate constant (h^{-1}), k_2 the pseudo-second rate constant ($g \cdot mg^{-1} \cdot h^{-1}$), a the sorption rate at the beginning of the process ($mg \cdot g^{-1} \cdot h^{-1}$), b is a coefficient related to the surface coverage and activation energy ($mg \cdot g^{-1}$), K_{id} is the intra-particle diffusion rate constant ($mg \cdot g^{-1} \cdot h^{-1/2}$) and C the intercept.

3. Results and discussion

3.1. Relation between contact time and diuron sorption

The apparent and true bulk densities were estimated to be 0.17 $g \cdot mL^{-1}$ ± 0.01 and 0.55 $g \cdot mL^{-1}$ ± 0.03, respectively, by Eq. (1). A pinewood porosity of 69.3 % ± 2.4 % was obtained using Eq. (2). These results are consistent with previous works (Kim et al., 2016; Vo et al., 1995).

Fig. 1 shows the curves of diuron sorption on pinewood chips over time. The system approached equilibrium in approximately 48 h for all sorbent amounts added (5, 10, 20, 30, 40, and 60 g). As expected, higher wood doses increased overall diuron elimination but decreased the saturation rate per unit of wood. Diuron sorption onto pine chips was mainly attributed to the chemical affinity that hydrophobic pesticides have for organic components of wood, such as lignin (Rodríguez-Cruz et al., 2009).

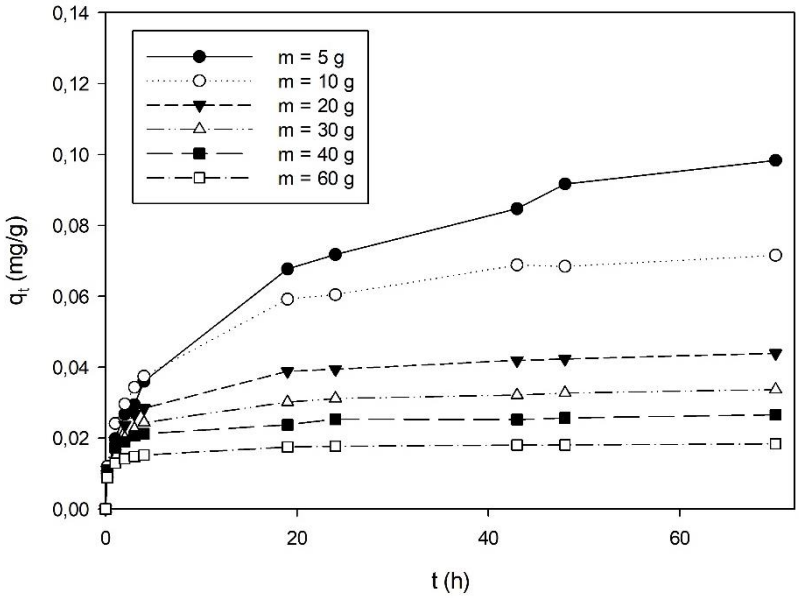

257

258 Fig. 1. Effect of contact time on diuron sorption for several sorbent doses at 25 ºC (C_0 =

259 6 mg·L^{-1})

260 Diuron was quickly sorbed onto external vacant sites at the beginning of the

261 experiment. Then, as the most superficial sites were filled, diuron molecules diffused

262 into the inner available sites of the chips, slowing the overall rate of sorption (Baccar et

263 al., 2012).

264 Table 1. Parameters, correlation coefficients and errors of Langmuir, Freundlich and

265 Temkin isotherm models for diuron sorption onto pinewood chips at 25 ºC

Isotherms	Parameters			
Langmuir	K_L (L·mg^{-1})	q_{max} (mg·g^{-1})	R^2	Δq (%)
Langmuir-1	0.057	0.548	0.993	5.782
Langmuir-2	0.046	0.677	0.423	5.758
Langmuir-3	0.112	0.305	0.387	7.200
Langmuir-4	0.043	0.711	0.387	5.789
Langmuir-5	0.051	0.610	0.993	5.757

Freundlich	n	q_{max} (mg·g^{-1})	R^2	Δq (%)
	1.085	0.154	0.993	5.245
Temkin	A	B	R^2	Δq (%)
	2.113	0.044	0.938	13.637

Significantly lower q_t values were obtained compared to other studies using similar carbon-based materials (De Gisi et al., 2016). However, this result was attributed to the higher wood-wastewater mass ratio used in the present work.

3.2. Sorption isotherms

The experimental equilibrium data were fitted to several isotherm models, which describe possible sorption mechanisms and facilitate the subsequent design of the sorption process. The Langmuir, Freundlich and Temkin models were investigated. The isotherm equations were also linearized and plotted to determine the most representative model and its characteristic parameters from the slope and intercept. Five different Langmuir linear forms were used since significant variations in their fits and parameter values were previously reported (Baccar et al., 2013). The linear forms of the isotherms are available in Table S1 of the Supplementary material.

The Langmuir model proposes sorption on finite sites and the formation of a single monolayer without chemical interaction among sorbate molecules. Moreover, the empirical Freundlich model considers sorption on heterogeneous surfaces and is more suitable for low concentrations (Appel, 1973). Finally, the Temkin isotherm model assumes chemical interactions among molecules and a linear decrease in binding energy as vacant sites are filled.

The linear correlation coefficient R^2 and the normalized standard deviation Δq (%) were used to evaluate the correlation between the experimental data and the sorption isotherms. Δq is described by Eq. (13).

$$\Delta q(\%) = 100\sqrt{\frac{\sum\left(\frac{q_{exp}-q_{cal}}{q_{exp}}\right)^2}{N-1}} \quad (13)$$

where q_{exp} and q_{cal} are the experimental and calculated amounts of diuron sorbed at equilibrium, respectively, and N is the number of measurements. A higher R^2 indicates a better fit between the linear form and the experimental data. Furthermore, a lower Δq represents a stronger correlation between the experimental and predicted data (Baccar et al., 2013).

Table 1 summarizes the main parameters and fit coefficients of the isotherm models. Although Langmuir-1, Langmuir-5 and Freundlich presented the highest R^2 (0.993), the Freundlich model exhibited a slightly lower Δq (5.245 %) and was thus considered to be the best model describing the equilibrium data. The Freundlich isotherm has been selected to represent pesticide sorption on carbon-based sorbents in previous studies (Laohaprapanon et al., 2010; Rodriguez-Cruz et al., 2007). Regarding the Freundlich parameters, a significantly low q_{max} of 0.154 mg·g^{-1} was estimated with Eq. (7), but this value was in good agreement with those reported in the literature (Iqbal and Ashiq, 2007). Nevertheless, a further discussion of the resulting q_{max} is proposed in Section 3.4. The parameter 1/n is related to the sorption susceptibility of the system and can indicate favourable (0 < 1/n <1), difficult (1/n > 1) or irreversible sorption (1/n = 0) (Yang et al., 2017). In this case, 1/n revealed favourable sorption (1/n = 0.922) of diuron onto pinewood chips.

3.3. Sorption kinetics

Sorption kinetics provide valuable information, such as the solute uptake rate and the reaction pathway, which allows the subsequent design and scale-up of a sorption system. The pseudo-first- and pseudo-second-order, intraparticle diffusion (IPD) and Elovich models were tested. The kinetic linear and non-linear equations of these models are shown in Table S2 of the Supplementary material. The pseudo-first and pseudo-second-order models consider chemisorption to be the dominant mechanism. In contrast, the IPD model identifies diffusion as the rate-limiting step. Between these two opposing models, the Elovich model describes intermediate behaviour with no clearly dominant mechanism (Wu et al., 2009).

The linear forms of these models were plotted to obtain the particular parameters of each model from the slope and the intercept. The best correlation to the experimental data was again selected according to R^2 and Δq. The fitting results for the kinetic models are presented in Table S3 of the Supplementary material. Although the pseudo-second order model gave the highest R^2 fits for all sorbent doses, the Elovich model more accurately described the experimental data based on Δq. The sole exception was for m = 5 g; in this case, the IPD model showed a better fit. Nevertheless, this result could be because the system did not fully reach equilibrium for m = 5 g in the period of time under study. It is probable that with a longer period of time, the system would reach complete equilibrium, and the Elovich model would provide the best fit. The Elovich model is appropriate for heterogeneous sorbents and liquid-solid systems, and it recognizes the effect of surface coverage on the sorption rate over time. Moreover, the values of the kinetic parameters are in agreement with previous studies of micropollutant sorption on porous carbon-based materials (Emeniru et al., 2017; Tseng et al., 2003).

3.4. Effect of successive sorption cycles on the sorption capacity

Successive sorption experiments were performed to verify the real sorption capacity of pinewood and to compare it to the q_{max} predicted by the Freundlich model. In addition, this system can represent real scenarios of sorption processes in continuous mode, with low solute concentrations and high sorbent doses. In this study, seven cycles in batch mode were completed by retaining the initial 20 g of pinewood chips and re-suspending the chips in 0.2 L new spiked wastewater at 8 ppm. The cumulative sorption of diuron is shown in Fig. 2.

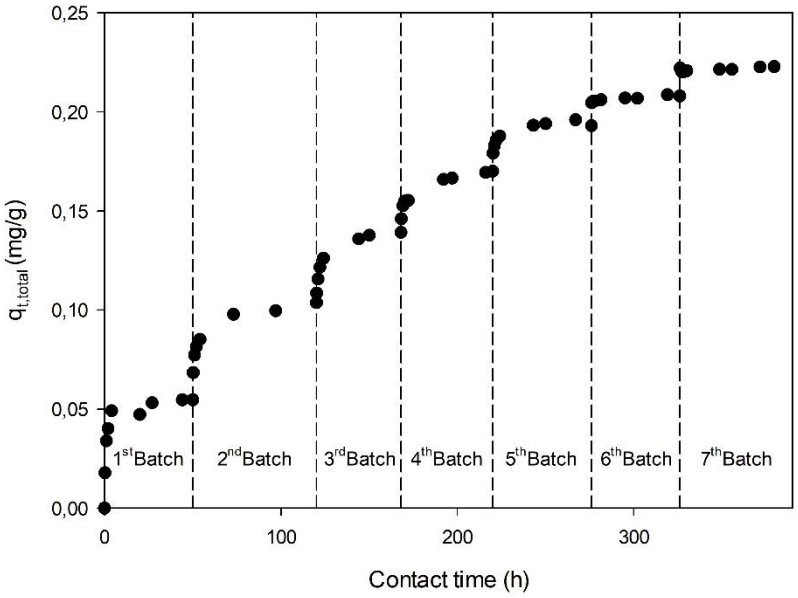

Fig. 2. Effect of repetitive cycles in batch on diuron sorption over contact time

In this case, a higher concentration of 8 ppm instead of 6 ppm was used to guarantee diuron detection in the HPLC (lower limit of detection of 0.5 ppm). As expected, increasing the initial diuron concentration led to higher sorption on the wood chips compared to that in the batch sorption process presented in Section 3.1 (0.05 instead of 0.04 $mg \cdot g^{-1}$). Once equilibrium was reached in the first batch of the successive sorption experiment, the treated wastewater was discarded, and a new 0.2 L sample of wastewater spiked with 8 ppm diuron was poured inside the same Erlenmeyer flask to start the second batch. In the second batch, the wood could sorb more diuron from the wastewater. This result indicated that the wood had reached equilibrium in the first

batch but its sorption capacity was not exhausted. The same process was repeated for 7 cycles. Although the sorption capacity of the wood was reduced with each new cycle, the wood was not completely saturated after 7 cycles.

Note that the Freundlich model estimated a q_{max} of 0.154 $mg \cdot g^{-1}$, but this level was exceeded after 4 cycles. The Freundlich model was initially selected because it provided the best fit based on the R (0.993) and Δq (5.757 %) values obtained in the batch experiment. However, the results of the successive batch process revealed that the Freundlich model could not accurately predict q_{max}. In fact, q_{max} is conventionally determined from the Langmuir model instead of by applying Eq. (7) to the Freundlich model (Baccar et al., 2013). In this study, the Langmuir model (Langmuir-5) obtained the same R and a Δq (5.245 %) insignificantly higher than that in the Freundlich model in the batch experiment. Since the Langmuir model showed a suitable fit, its estimated q_{max} was also compared to the experimental data. Langmuir-5 provided a q_{max} of 0.610 $mg \cdot g^{-1}$, which was more consistent with the findings of the successive sorption experiment. For that reason, the Langmuir and not the Freundlich model was selected as the most representative isotherm for the sorption system.

3.5. Packed-bed channel bioreactor treating diuron in spiked tap water

The PBCB was proposed as an alternative technology to the trickling packed-bed reactor used by Torán et al. (Torán et al., 2017) to facilitate future applications in crop fields. Continuous long-term treatment was initially conducted with spiked tap water to evaluate diuron removal under relatively aseptic conditions. Tap water was spiked with 10 ppm diuron to allow the detection of the remaining diuron by HPLC. Two channels were operated in parallel with the same initial conditions. One channel was loaded with wood chips to evaluate the contribution of the sorption process. The other channel was filled with wood chips previously colonized by *T. versicolor*. The biodegradation effect was deduced by comparing the control and the inoculated PBCBs.

377 Fig. 3 shows the diuron removals for both the control and inoculated PBCBs. White
378 columns represent the overall removals obtained in the control PBCB, while the sum of
379 the white and grey bars shows the overall removals in the inoculated PBCB. Grey
380 columns indicate biodegradation at each time. Biodegradation rates were calculated as
381 the differences between the overall removals of the control and the inoculated PBCBs.

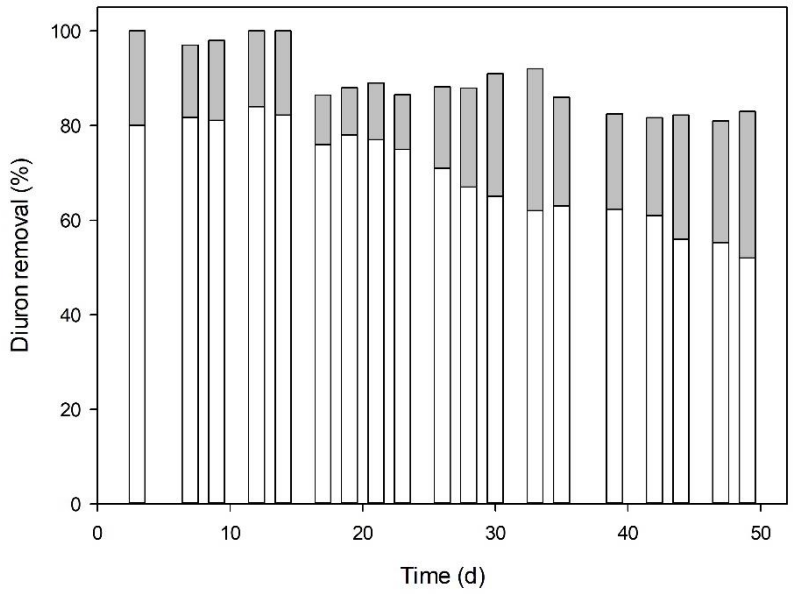

382

383 Fig 3. Relative removal profiles of diuron in the PBCB for spiked tap water. In white,
384 diuron elimination in the control reactor. The entire columns (sum of the white and grey
385 columns) represent the overall removals of the inoculated bioreactor. In grey, the
386 biodegradation contribution obtained in the inoculated bioreactor. In all cases, errors of
387 less than 3 % diuron removal were obtained (standard deviation of triplicates).

388 The average diuron removals were 89 ± 4 % and 69 ± 11 % after 49 d for the
389 inoculated and control reactors, respectively (Fig. 3). There was overall 20 % higher
390 diuron removal in the inoculated channel, which was associated with fungal
391 bioremediation, as indicated by the grey column portions in Fig. 3. In addition, the
392 diuron removal trend showed a more pronounced decline in the case of the control
393 channel, which can be observed in the removal evolution over time in Fig. 3. In fact, an

even higher removal difference was observed at the end of the treatment, reaching up to 30 % more elimination in the case of the inoculated channel.

In this experiment, the wood substrate served not only as a single source of nutrients for *T. versicolor* but also as a support for fungus immobilization and as an effective sorbent for diuron removal. In addition, the wood substrate provided enough nutrients to ensure fungus survival and the co-metabolic biodegradation of diuron (Liang Jiwei Wen Dawen Gao, 2011; Mir-Tutusaus et al., 2018).

3.6. Packed-bed channel bioreactor treating diuron in spiked real wastewater

The same system used in Section 3.5 was employed to treat real wastewater spiked with diuron (10 ppm) to evaluate the effect of a real matrix on the removal rate of the inoculated system. No interference was observed between the HPLC chromatograms of the spiked tap water and spiked real wastewater. No diuron (above 0.5 ppm) was initially detected in the original wastewater matrix. Fig. 4 shows the evolution of the diuron removal over time. An average diuron removal of 94 ± 5 % was obtained for the inoculated reactor during 35 d of treatment. In this case, the same removal results obtained for the control reactor in the tap water treatment were used to represent the control contribution in the wastewater treatment (see Fig. 4), since negligible variations were expected (Mahmoud et al., 2016). A significant difference in diuron removal was detected between the inoculated and control reactors throughout the treatment, and it was attributed to biodegradation by *T. versicolor*. Note that the maximum removal divergence was obtained at the end of the process, when the sorption capacity was considerably reduced for the control reactor but the elimination rate of the inoculated reactor remained stable.

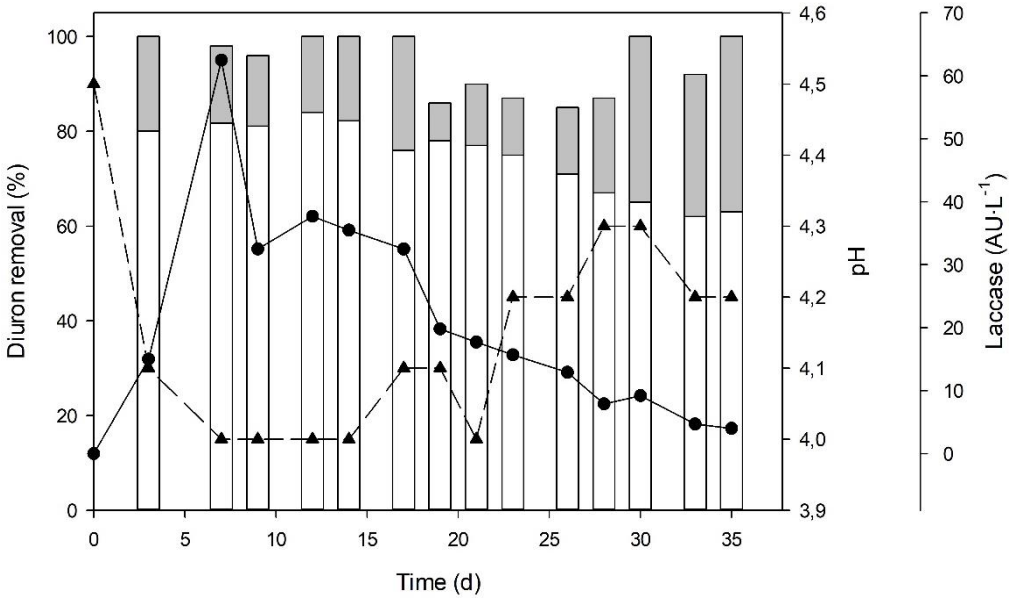

Fig. 4. Relative removal profiles of diuron in the PBCB for spiked wastewater. In white colour, diuron elimination in the control reactor. The entire columns (sum of the white and grey columns) represent the overall removals of the inoculated bioreactor. In grey, the biodegradation contribution obtained in the inoculated bioreactor. The pH and laccase levels are indicated with triangles and circles, respectively. In all cases, errors of less than 3 % diuron removal and 2 % laccase level were obtained (standard deviation of triplicates).

Higher diuron degradation was obtained in the wastewater treatment compared to the tap water experiment. This difference was attributed to synergistic cooperation between autochthonous microorganisms in the wastewater and *T. versicolor*. Similarly, Ellegaard-Jensen et al. (Ellegaard-Jensen et al., 2014) demonstrated that the cooperative catabolism of certain fungal-bacterial consortia improved the degradation efficiency of diuron.

In addition, the laccase level was monitored as an indicator of the enzymatic activity of *T. versicolor*. A laccase peak of 62 $AU \cdot L^{-1}$ was detected on the 5th day and then decayed to approximately 30 $AU \cdot L^{-1}$ and 4 $AU \cdot L^{-1}$ after 17 and 35 d, respectively. However, the degradation profile of diuron did not follow the same negative trend,

436 indicating that laccase was probably not involved in the degradation of this pesticide
437 (Coelho-Moreira et al., 2013).

438 A pH of 7.9 was initially measured for the real wastewater. Since the optimal pH range
439 for *T. versicolor* is between 4.3 and 4.7, the pH of the influent tank was initially adjusted
440 to 4.5. However, *T. versicolor* progressively acidified the medium (Tavares et al., 2006)
441 to 3.8 at day 11. Consequently, the pH of the inlet was increased to 5.5 to maintain the
442 optimal pH range in the channel. However, the pH again decreased below the lower
443 limit of the optimal range for the fungus at day 21, and the pH of the influent was
444 readjusted to 6.5 until the end of the treatment to maintain a pH of approximately 4.5.

445 No significant differences in absorbance, CFU number, ammonia concentration, TSS or
446 COD were observed during the treatment (Table S4 of the Supplementary material).
447 The development of bacterial communities is considered a critical point in fungal
448 treatments (Yang et al., 2013), but fungal immobilization on pine chips proved to be an
449 excellent technique to deal with bacterial growth, preventing fungal inhibition.

450 The PBCB of pinewood colonized by *T. versicolor* showed high efficiency of diuron
451 removal in a continuous long-term treatment. Although manual mixing of inoculated
452 wood chips was a good strategy to preserve aerobic conditions and thus the enzymatic
453 activity and degradation capacity of *T. versicolor*, this step should be substituted by an
454 automated system.

455 **3.7. Rotating drum bioreactor treating diuron in spiked real wastewater**

456 Based on the excellent performance shown by the PBCB, an RDB was proposed to
457 automatize the treatment process. Manual mixing was replaced by continuous and
458 automatized rotation of the RDB internal tube, which was provided by an electric motor.
459 In addition, the output pumps were discarded, and the effluent left the reactor by
460 overflow. Fungal RDBs have been previously used for enzyme production (Colla et al.,

2017; Domínguez et al., 2001) and biological desulfurization (Şener et al., 2018), and a similar rotating drum biological contactor of *white-rot fungus* has been applied for decolorization (Šíma et al., 2016). Recently, rotating biological contactors containing immobilized *T. versicolor* were implemented to remove pharmaceutical micropollutants from urban wastewaters (Cruz del Álamo et al., 2020). However, this is the first time that a fungal RDB has been used for micropollutant treatment of real wastewaters. An incubation time of 9 d was required to completely cover the wood surface with T. versicolor before using the immobilized fungus in the PBCB. A higher incubation time was used in the RDB (20 d) compared to the PBCB (9 d) to improve fungal immobilization.

Continuous agitation at 6 rpm was initially employed to ensure enough oxygen diffusion and perfect mixing inside the tube-shaped reactor. However, *T. versicolor* was progressively detached from the wood surface during treatment, probably due to the generation of significant shear forces that damaged the mycelial structure of the fungus (Zhong, 2010). This fact indicated that the rotation speed was too high to maintain fungal immobilization on the pinewood over time. The rotation speed also produced foam inside the inoculated reactor, which has been identified as a major issue in fungal treatments (Espinosa-Ortiz et al., 2016).

Nonetheless, the average diuron elimination was again slightly higher for the inoculated reactor (61 % ± 3 %) than for the control reactor (55 % ± 7 %), as shown in Fig. 5. Diuron removal decreased over time for the control reactor, which was probably due to wood saturation (Torán et al., 2017). In contrast, the removal rate of the inoculated reactor was more stable, remaining above 60 % after 16 d of treatment. A significant difference of up to 20 % in diuron removal was achieved at the end of the process. The process was stopped after 16 d because it seemed that *T. versicolor* had been significantly removed from the substrate surface.

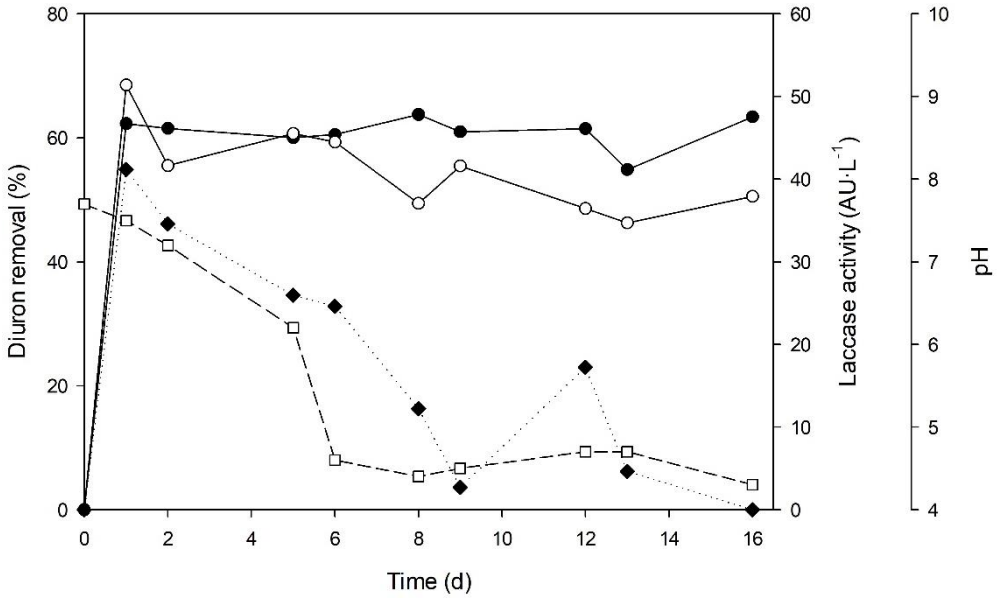

Figure 5. Diuron removal profiles for the inoculated (black dots) and the control (white dots) RBDs, laccase activity (black rhombuses) and pH evolution (white squares) for inoculated RDB. In all cases, errors of less than 3 % diuron removal and 2 % laccase level were obtained (standard deviation of triplicates).

A lower mean removal was observed compared to that obtained with the PBCB, even between the control reactors. This difference was mainly attributed to the different wood/wastewater doses used between the PBCBs and the RBDs. For the RBDs, an almost 7 times lower dose was used (152 $g \cdot L^{-1}$), but diuron removal did not decrease proportionally, and only a mean reduction of 14 % was obtained between the control reactors. This difference was probably due to the more efficient contact between the wood chips and the wastewater driven by the continuous rotation. It has been demonstrated that the agitation speed modifies not only the sorption kinetics but also the sorption equilibrium of organic compounds on carbon-based materials (Kuśmierek and Świątkowski, 2015). A higher removal efficiency was obtained by Torán et al. (Torán et al., 2017) when working with immobilized *T. versicolor* on pine chips in a packed bed reactor for ibuprofen (90 %) and ketoprofen (80 %) removals, but a similar

504 removal efficiency was obtained for naproxen (60 %). Nevertheless, in that case, a
505 higher dose of 240 g wood·L^{-1} wastewater was also employed.

506 Laccase was measured as an indicator of fungal activity, and it was reduced from 41
507 AU·L^{-1} to almost zero after 16 d. However, the lack of laccase was not accompanied by
508 lower elimination rates of diuron over time. This result is quite typical in fungal
509 treatments because cytochrome P450 generally plays a more important role in the
510 degradation of micropollutants (Marco-Urrea et al., 2009). Similar laccase levels and
511 evolution over time were also detected by Torán et al. when working with *Trametes*
512 *versicolor* immobilized on wood chips (Torán et al., 2017).

513 The initial pH of the wastewater was not adjusted for the RDB at the beginning of the
514 treatment. This decision was based on the natural ability of *T. versicolor* to acidify the
515 medium observed during the PBCB experiment. As shown in Fig. 5, the pH was
516 progressively reduced during the first days of the process. However, pH control was
517 established in the range of 4.3 to 4.7 on day 5 to ensure optimal operational conditions
518 for *T. versicolor* to reverse and attenuate the fungal losses derived from the high
519 rotation speed.

520 The HPC increase for the RDB was slightly higher than that for the PBCB; HPC rose
521 from an initial $4.8 \cdot 10^4 \pm 2.7 \cdot 10^4$ CFU·mL^{-1} to $5.4 \cdot 10^5 \pm 5.0 \cdot 10^4$ CFU·mL^{-1} after 16 d
522 (Table S5, Supplementary material). This greater bacterial proliferation was probably
523 associated with both the lower wood/wastewater dose employed in the RDB and the
524 superficial removal of *T. versicolor* from the pinewood chips. Mir-Tutusaus et al. (Mir-
525 Tutusaus et al., 2016) obtained a 100-fold increase in HPC after only 3 d of treating
526 non-sterile hospital wastewater with *T. versicolor* in a fluidized reactor. This notable
527 increase was promoted by the addition of glucose and NH_4Cl as the main source of
528 nutrients for the fungus, since these compounds are easily assimilable by bacteria. A
529 more moderate increase in HPC was achieved in continuous mode with a preliminary

coagulation-flocculation step, which implies higher operational costs. In the present study, the HPC increase was limited, and costs associated with nutrient supply and pre-treatment were completely avoided.

4. Conclusions

Trametes versicolor immobilized on wood chips was used to treat agricultural wastewaters in simple channel bioreactors. According to the sorption isotherm, the Freundlich model gave the best fit for diuron sorption on the wood chips. However, successive sorption experiments revealed inconsistencies between the q_{max} predicted by the Freundlich model and the experimental results. In contrast, the experimental data conformed to the q_{max} predicted by the Langmuir model, and thus, the Langmuir model was selected as the most representative one. Regarding kinetics, the Elovich model showed the best fit, suggesting that no sorption mechanism was predominant. The PBCB showed high diuron removal from agricultural wastewater. Moreover, synergistic interactions between *T. versicolor* and indigenous microorganisms were proven. The automated RDB effectively removed diuron from spiked real wastewater requiring 7 times lower wood amount than the PBCB. Further research should explore in depth the effect of the main process variables on the removal efficiency, analyse complex mixtures of pesticides at real concentrations, use mixtures of wood substrates, and finally scale up the process.

Acknowledgements

This work has been supported by the Spanish Ministry of Economy and Competitiveness State Research Agency (CTM2016-75587-C2-1-R) co-financed by the European Union through the European Regional Development Fund (ERDF). This work was partly supported by the Generalitat de Catalunya (Consolidate Research Group 2017-SGR-14). The Department of Chemical, Biological and Environmental

555 Engineering of the Universitat Autònoma de Barcelona is a member of the Xarxa de
556 Referència en Biotecnologia de la Generalitat de Catalunya. Eduardo Beltrán-Flores
557 acknowledges support from a MINECO predoctoral research grant (BES-2017-
558 080500).

559 **References**

560 APHA, 1995. Standard Methods for the Examination of Water and Wastewater,
561 American Public Association/AmericaWaterWorks Association/ Water Water
562 Environment Federation, Washington.

563 Appel, J., 1973. Freundlich's adsorption isotherm. Surf. Sci. 39, 237–244.
564 https://doi.org/10.1016/0039-6028(73)90105-2

565 Asgher, M., Bhatti, H.N., Ashraf, M., Legge, R.L., 2008. Recent developments in
566 biodegradation of industrial pollutants by white rot fungi and their enzyme system.
567 Biodegradation 19, 771–783. https://doi.org/10.1007/s10532-008-9185-3

568 ASTM, 2018. ASTM D7481-18 Standard Test Methods for Determining Loose and
569 Tapped Bulk Densities of Powders using a Graduated Cylinder, ASTM
570 International, West Conshohocken.

571 Baccar, R., Blánquez, P., Bouzid, J., Feki, M., Attiya, H., Sarrà, M., 2013. Modeling of
572 adsorption isotherms and kinetics of a tannery dye onto an activated carbon
573 prepared from an agricultural by-product. Fuel Process. Technol. 106, 408–415.
574 https://doi.org/10.1016/j.fuproc.2012.09.006

575 Baccar, R., Sarrà, M., Bouzid, J., Feki, M., Blánquez, P., 2012. Removal of
576 pharmaceutical compounds by activated carbon prepared from agricultural by-
577 product. Chem. Eng. J. 211–212, 310–317.
578 https://doi.org/10.1016/j.cej.2012.09.099

579 Badia-Fabregat, M., Lucas, D., Pereira, M.A., Alves, M., Pennanen, T., Fritze, H.,
580 Rodríguez-Mozaz, S., Barceló, D., Vicent, T., Caminal, G., 2016. Continuous
581 fungal treatment of non-sterile veterinary hospital effluent: pharmaceuticals
582 removal and microbial community assessment. Appl. Microbiol. Biotechnol. 100,
583 2401–2415. https://doi.org/10.1007/s00253-015-7105-0

584 Blanquez, P., Casas, N., Font, X., Gabarrell, X., Sarrá, M., Caminal, G., Vicent, T.,
585 2004. Mechanism of textile metal dye biotransformation by Trametes versicolor.
586 Water Res. 38, 2166–2172. https://doi.org/10.1016/j.watres.2004.01.019

587 Blánquez, P., Sarrà, M., Vicent, M.T., 2006. Study of the cellular retention time and the
588 partial biomass renovation in a fungal decolourisation continuous process. Water
589 Res. 40, 1650–1656. https://doi.org/10.1016/j.watres.2006.02.010

590 Cabana, H., Jiwan, J.L.H., Rozenberg, R., Elisashvili, V., Penninckx, M., Agathos, S.N.,
591 Jones, J.P., 2007. Elimination of endocrine disrupting chemicals nonylphenol and
592 bisphenol A and personal care product ingredient triclosan using enzyme
593 preparation from the white rot fungus Coriolopsis polyzona. Chemosphere 67,
594 770–778. https://doi.org/10.1016/j.chemosphere.2006.10.037

595 Ccanccapa, A., Masiá, A., Navarro-Ortega, A., Picó, Y., Barceló, D., 2016. Pesticides
596 in the Ebro River basin: Occurrence and risk assessment. Environ. Pollut. 211,
597 414–424. https://doi.org/10.1016/j.envpol.2015.12.059

598 Coelho-Moreira, J.D.S., Bracht, A., Da Silva De Souza, A.C., Oliveira, R.F., Sá-
599 Nakanishi, A.B. De, Souza, C.G.M. De, Peralta, R.M., 2013. Degradation of diuron
600 by phanerochaete chrysosporium: Role of ligninolytic enzymes and cytochrome
601 P450. Biomed Res. Int. 2013. https://doi.org/10.1155/2013/251354

602 Colla, E., Santos, L.O., Deamici, K., Magagnin, G., Vendruscolo, M., Costa, J.A.V.,
603 2017. Simultaneous Production of Amyloglucosidase and Exo-Polygalacturonase

by Aspergillus niger in a Rotating Drum Reactor. Appl. Biochem. Biotechnol. 181, 627–637. https://doi.org/10.1007/s12010-016-2237-y

Cruz-Morató, C., Ferrando-Climent, L., Rodriguez-Mozaz, S., Barceló, D., Marco-Urrea, E., Vicent, T., Sarrà, M., 2013. Degradation of pharmaceuticals in non-sterile urban wastewater by Trametes versicolor in a fluidized bed bioreactor. Water Res. 47, 5200–5210.

Cruz del Álamo, A., Pariente, M.I., Martínez, F., Molina, R., 2020. Trametes versicolor immobilized on rotating biological contactors as alternative biological treatment for the removal of emerging concern micropollutants. Water Res. 170.

De Gisi, S., Lofrano, G., Grassi, M., Notarnicola, M., 2016. Characteristics and adsorption capacities of low-cost sorbents for wastewater treatment: A review. Sustain. Mater. Technol. https://doi.org/10.1016/j.susmat.2016.06.002

Ding, J., Chen, B.L., Zhu, L.Z., 2013. Biosorption and biodegradation of polycyclic aromatic hydrocarbons by Phanerochaete chrysosporium in aqueous solution. Chinese Sci. Bull. 58, 613–621. https://doi.org/10.1007/s11434-012-5411-9

Domínguez, A., Rivela, I., Couto, S.R., Sanromán, M.Á., 2001. Design of a new rotating drum bioreactor for ligninolytic enzyme production by Phanerochaete chrysosporium grown on an inert support. Process Biochem. 37, 549–554. https://doi.org/10.1016/S0032-9592(01)00233-3

Ellegaard-Jensen, L., Knudsen, B.E., Johansen, A., Albers, C.N., Aamand, J., Rosendahl, S., 2014. Fungal-bacterial consortia increase diuron degradation in water-unsaturated systems. Sci. Total Environ. 466–467, 699–705. https://doi.org/10.1016/j.scitotenv.2013.07.095

Emeniru, D.C., Adubazi, M.O., Wodu, P.-E.D., Dieware, G.K., 2017. Benzene Uptake

628 onto Modified Tea Waste: Perspective Applicability of Empirical Sorption Kinetic
629 Models. Eur. Sci. J. 206–232. https://doi.org/10.19044/esj.2017.c1p17

630 Espinosa-Ortiz, E.J., Rene, E.R., Pakshirajan, K., Van Hullebusch, E.D., Lens, P.N.L.,
631 2016. Fungal pelleted reactors in wastewater treatment: Applications and
632 perspectives. Chem. Eng. J. 283, 553–571.
633 https://doi.org/10.1016/j.cej.2015.07.068

634 European Commission, 2007. Commission Decision of 13 June 2007 concerning the
635 non-inclusion of diuron in Annex I to Council Directive 91/414/EEC and the
636 withdrawal of authorisations for plant protection products containing that
637 substance (2007/417/EC).

638 European Commission, 2000. Directive 2000/60/EC of the European Parlament and of
639 the Council of 23 October 2000 establishing a framework for Community action in
640 the field of water policy, Official Journal of the European Communities.

641 European Commission, 1998. Directive on the quality of water intended human
642 consumption (98/83/EC). Official Journal of European Communities, No L330/32.
643 Commission of the European Communities, Brussels.

644 Giacomazzi, S., Cochet, N., 2004. Environmental impact of diuron transformation: A
645 review. Chemosphere. https://doi.org/10.1016/j.chemosphere.2004.04.061

646 Haroune, L., Saibi, S., Bellenger, J.P., Cabana, H., 2014. Evaluation of the efficiency of
647 Trametes hirsuta for the removal of multiple pharmaceutical compounds under low
648 concentrations relevant to the environment. Bioresour. Technol. 171, 199–202.
649 https://doi.org/10.1016/j.biortech.2014.08.036

650 Huovinen, M., Loikkanen, J., Naarala, J., Vähäkangas, K., 2015. Toxicity of diuron in
651 human cancer cells. Toxicol. Vitr. 29, 1577–1586.

652 https://doi.org/http://dx.doi.org/10.1016/j.tiv.2015.06.013

653 Iqbal, M.J., Ashiq, M.N., 2007. Adsorption of dyes from aqueous solutions on activated
654 charcoal. J. Hazard. Mater. 139, 57–66.
655 https://doi.org/10.1016/j.jhazmat.2006.06.007

656 Jury, W.A., Spencer, W.F., Farmer, W.J., 1983. Behavior Assessment Model for Trace
657 Organics in Soil : III . Application of Screening Model. J. Environ. Qual. 13, 573–
658 579.

659 Kim, J.S., Jung, J.Y., Ha, S.Y., Yang, J.K., 2016. Physicochemical properties and
660 growth characteristics of wood chip and peat moss based vegetation media. J.
661 Korean Wood Sci. Technol. 44, 323–336.
662 https://doi.org/10.5658/WOOD.2016.44.3.323

663 Kuśmierek, K., Świątkowski, A., 2015. The influence of different agitation techniques on
664 the adsorption kinetics of 4-chlorophenol on granular activated carbon. React.
665 Kinet. Mech. Catal. 116, 261–271. https://doi.org/10.1007/s11144-015-0889-1

666 Langeron, J., Sayen, S., Couderchet, M., Guillon, E., 2014. Leaching potential of
667 phenylurea herbicides in a calcareous soil: Comparison of column elution and
668 batch studies. Environ. Sci. Pollut. Res. 21, 4906–4913.
669 https://doi.org/10.1007/s11356-012-1244-y

670 Laohaprapanon, S., Marques, M., Hogland, W., 2010. Removal of organic pollutants
671 from wastewater using wood fly ash as a low-cost sorbent. Clean - Soil, Air, Water
672 38, 1055–1061. https://doi.org/10.1002/clen.201000105

673 Lapworth, D.J., Gooddy, D.C., 2006. Source and persistence of pesticides in a semi-
674 confined chalk aquifer of southeast England. Environ. Pollut. 144, 1031–1044.
675 https://doi.org/10.1016/j.envpol.2005.12.055

676 Li, X., Xu, J., de Toledo, R.A., Shim, H., 2015. Enhanced removal of naproxen and
677 carbamazepine from wastewater using a novel countercurrent seepage bioreactor
678 immobilized with Phanerochaete chrysosporium under non-sterile conditions.
679 Bioresour. Technol. 197, 465–474.

680 Liang Jiwei Wen Dawen Gao, H., 2011. Cometabolic degradation of pyrene by
681 indigenous white-rot fungi Pseudotrametes gibbosa, in: ACS National Meeting
682 Book of Abstracts. https://doi.org/10.1016/j.ibiod.2011.03.003

683 Mahmoud, M.E., Nabil, G.M., El-Mallah, N.M., Karar, S.B., 2016. Assessment of the
684 adsorptive color removal of methylene blue dye from water by activated carbon
685 sorbent-immobilized-sodium decyl sulfate surfactant. Desalin. Water Treat. 57,
686 8389–8405. https://doi.org/doi: 10.1080/19443994.2015.1019367

687 Marco-Urrea, E., Pérez-Trujillo, M., Vicent, T., Caminal, G., 2009. Ability of white-rot
688 fungi to remove selected pharmaceuticals and identification of degradation
689 products of ibuprofen by Trametes versicolor. Chemosphere 74, 765–772.
690 https://doi.org/10.1016/j.chemosphere.2008.10.040

691 Marican, A., Durán-Lara, E.F., 2018. A review on pesticide removal through different
692 processes. Environ. Sci. Pollut. Res. 25, 2051–2064.
693 https://doi.org/10.1007/s11356-017-0796-2

694 Mir-Tutusaus, J.A., Baccar, R., Caminal, G., Sarrà, M., 2018. Can white-rot fungi be a
695 real wastewater treatment alternative for organic micropollutants removal? A
696 review. Water Res. 138, 137–151. https://doi.org/10.1016/j.watres.2018.02.056

697 Mir-Tutusaus, J.A., Masís-Mora, M., Corcellas, C., Eljarrat, E., Barceló, D., Sarrà, M.,
698 Caminal, G., Vicent, T., Rodríguez-Rodríguez, C.E., 2014. Degradation of
699 selected agrochemicals by the white rot fungus Trametes versicolor. Sci. Total
700 Environ. 500–501, 235–242. https://doi.org/10.1016/j.scitotenv.2014.08.116

701 Mir-Tutusaus, J.A., Sarrà, M., Caminal, G., 2016. Continuous treatment of non-sterile
702 hospital wastewater by Trametes versicolor: How to increase fungal viability by
703 means of operational strategies and pretreatments. J. Hazard. Mater. 318, 561–
704 570. https://doi.org/http://dx.doi.org/10.1016/j.jhazmat.2016.07.036

705 Palma, P., Köck-Schulmeyer, M., Alvarenga, P., Ledo, L., Barbosa, I.R., López de
706 Alda, M., Barceló, D., 2014. Risk assessment of pesticides detected in surface
707 water of the Alqueva reservoir (Guadiana basin, southern of Portugal). Sci. Total
708 Environ. 488–489, 208–219. https://doi.org/10.1016/j.scitotenv.2014.04.088

709 Prieto-Rodriguez, L., Miralles-Cuevas, S., Oller, I., Agüera, A., Puma, G.L., Malato, S.,
710 2012. Treatment of emerging contaminants in wastewater treatment plants
711 (WWTP) effluents by solar photocatalysis using low TiO 2 concentrations. J.
712 Hazard. Mater. 211–212, 131–137. https://doi.org/10.1016/j.jhazmat.2011.09.008

713 Rodarte-Morales, A.I., Feijoo, G., Moreira, M.T., Lema, J.M., 2011. Degradation of
714 selected pharmaceutical and personal care products (PPCPs) by white-rot fungi.
715 World J. Microbiol. Biotechnol. 27, 1839–1846. https://doi.org/10.1007/s11274-
716 010-0642-x

717 Rodríguez-Cruz, M.S., Valderrábano, M., Del Hoyo, C., Sánchez-Martín, M.J., 2009.
718 Physicochemical study of the sorption of pesticides by wood components. J.
719 Environ. Qual. 38, 719–728. https://doi.org/10.2134/jeq2008.0150

720 Rodriguez-Cruz, S., Andrades, M.S., Sanchez-Camazano, M., Sanchez-Martin, M.J.,
721 2007. Relationship between the adsorption capacity of pesticides by wood
722 residues and the properties of woods and pesticides. Environ. Sci. Technol. 41,
723 3613–3619. https://doi.org/10.1021/es062616f

724 Rupp, D.E., Peachey, R.E., Warren, K.L., Selker, J.S., 2006. Diuron in surface runoff
725 and tile drainage from two grass-seed fields. J. Environ. Qual. 35, 303–311.

https://doi.org/10.2134/jeq2005.0093

Şener, B., Aksoy, D.Ö., Çelik, P.A., Toptaş, Y., Koca, S., Koca, H., Çabuk, A., 2018. Fungal treatment of lignites with higher ash and sulphur contents using drum type reactor. Hydrometallurgy 182, 64–74. https://doi.org/10.1016/j.hydromet.2018.10.017

Šíma, J., Pocedič, J., Hasal, P., 2016. Decolorization of Reactive Orange 16 in Rotating Drum Biological Contactor. J. Environ. Chem. Eng. 4, 4540–4548. https://doi.org/10.1016/j.jece.2016.10.010

Taheran, M., Brar, S.K., Verma, M., Surampalli, R.Y., Zhang, T.C., Valero, J.R., 2016. Membrane processes for removal of pharmaceutically active compounds (PhACs) from water and wastewaters. Sci. Total Environ. 547, 60–77. https://doi.org/10.1016/j.scitotenv.2015.12.139

Tavares, A.P.M., Coelho, M.A.Z., Agapito, M.S.M., Coutinho, J.A.P., Xavier, A.M.R.B., 2006. Optimization and modeling of laccase production by Trametes versicolor in a bioreactor using statistical experimental design. Appl. Biochem. Biotechnol. 134, 233–248. https://doi.org/10.1385/ABAB:134:3:233

Tixier, C., Sancleme, M., Bonnemoy, F., Cuer, A., Veschambre, H., 2001. Degradation products of a phenylurea herbicide, diuron: synthesis, ecotoxicity and biotransformation. Environ. Toxicol. Chem. 20, 1381–1389. https://doi.org/10.1897/1551-5028(2001)020<1381:dpoaph>2.0.co;2

Torán, J., Blánquez, P., Caminal, G., 2017. Comparison between several reactors with Trametes versicolor immobilized on lignocellulosic support for the continuous treatments of hospital wastewater. Bioresour. Technol. 243, 966–974. https://doi.org/10.1016/j.biortech.2017.07.055

750 Tseng, R.L., Wu, F.C., Juang, R.S., 2003. Liquid-phase adsorption of dyes and
751 phenols using pinewood-based activated carbons. Carbon N. Y. 41, 487–495.
752 https://doi.org/10.1016/S0008-6223(02)00367-6

753 US EPA, 2003. Reregistration Eligibility for Decision (RED) for diuron.

754 Vo, E. V, Ridis, U., Pa, N., Lis, S., 1995. Valorisation de différentes espèces
755 méditerranéennes. Characteristics and technological properties of the wood of
756 mediterranean evergreen hardwoods.

757 Wu, F.-C., Tseng, R.-L., Juang, R.-S., 2009. Characteristics of Elovich equation used
758 for the analysis of adsorption kinetics in dye-chitosan systems. Chem. Eng. J. 150,
759 366–373. https://doi.org/10.1016/j.cej.2009.01.014

760 Yang, Q., Wang, Jing, Zhang, W., Liu, F., Yue, X., Liu, Y., Yang, M., Li, Z., Wang,
761 Jianlong, 2017. Interface engineering of metal organic framework on graphene
762 oxide with enhanced adsorption capacity for organophosphorus pesticide. Chem.
763 Eng. J. 313, 19–26. https://doi.org/10.1016/j.cej.2016.12.041

764 Yang, S., Hai, F.I., Nghiem, L.D., Nguyen, L.N., Roddick, F., Price, W.E., 2013.
765 Removal of bisphenol A and diclofenac by a novel fungal membrane bioreactor
766 operated under non-sterile conditions. Int. Biodeterior. Biodegrad. 85, 483–490.
767 https://doi.org/10.1016/j.ibiod.2013.03.012

768 Zhong, J.J., 2010. Recent advances in bioreactor engineering. Korean J. Chem. Eng.
769 27, 1035–1041. https://doi.org/10.1007/s11814-010-0277-5

770